INTERNATIONAL JOURNAL OF ENERGY RESEARCH
Int. J. Energy Res. 2010; **34**:293–302
Published online 21 December 2009 in Wiley InterScience
(www.interscience.wiley.com). DOI: 10.1002/er.1662

A novel scheme for precise diagnostics and effective stabilization of currents in a fuel cell stack

J. A. Hirschfeld[1,*,†], H. Lustfeld[2], M. Reißel[3] and B. Steffen[4]

[1]*Forschungszentrum Jülich, IAS-1, Jülich, Germany*
[2]*Forschungszentrum Jülich, IFF-1, Jülich, Germany*
[3]*Fachhochschule Aachen, Abteilung Jülich, Jülich, Germany*
[4]*Forschungszentrum Jülich, JSC, Jülich, Germany*

SUMMARY

A novel scheme for detecting inhomogeneous internal currents in a fuel cell stack is presented. In this paper the scheme is investigated for the case that the flow field plates consist of graphite. Then plates of high conductivity, e.g. aluminium between the flow field plates together with small slits in these plates have three effects: (a) Whenever a local inhomogeneity of the electric current occurs at a particular cell in the stack, this will induce a surface current close to that cell perpendicular to the averaged current. This current can be detected. (b) The plates of high conductivity completely prevent the inhomogeneities from spreading to neighbouring cells. (c) Even at the particular cell the inhomogeneity is suppressed as far as possible. Thus this scheme leads to much better diagnostic possibilities and at the same time reduces electric instabilities to an extent, where they probably become harmless. This scheme will first be explained for a simple model to clarify the idea. However, very precise three dimensional computations using realistic parameters are presented, corroborating the results of the simple model. Copyright © 2009 John Wiley & Sons, Ltd.

KEY WORDS: defect detection; degradation; stack; operation stabilization; current density distribution; modelling; fuel cell; DMFC; PEMFC; MEA

1. INTRODUCTION

A single direct methanol fuel cell (DMFC) or proton exchange membrane fuel cell (PEMFC) contains the membrane electrode assembly (MEA) consisting of anode, electrolyte and cathode, furthermore on both sides of the MEA there are the flow field plates (typically consisting of steel or graphite [1]), in which the gases or liquids of the fuel as well as the exhaust gases are transported. As a single fuel cell can typically produce a voltage of about 0.3 V (DMFC), 0.7 V (PEMFC) to 0.9 V (solid oxide fuel cell (SOFC)) [2] only, several or many (about 100) fuel cells are connected—usually in series—forming a stack [3]. There are interesting modifications of how to connect fuel cells [4], but for simplicity we will restrict ourselves to the standard case.

*Correspondence to: J. A. Hirschfeld, Forschungszentrum Jülich, IAS-1, 52425 Jülich, Germany.
†E-mail: j.hirschfeld@fz-juelich.de

Received 24 April 2009
Revised 29 October 2009
Accepted 2 November 2009

It is a non-trivial engineering task to keep even a single fuel cell in a stable state [5] for a very long period of time even if the power requirements remain constant over that period. The efficiency depends on temperature, on humidity [6] in the polymeric electrolyte and on fuel as well as exhaust gas conditions [7–10]. All this can lead to irregularities in the local electric current density produced by the MEA. Therefore the local current density can differ by a factor of 1.5–3 in a single MEA [11–14]. And here lies a problem of the stack: an irregular electric current of one cell, still harmless for this cell, may accumulate due to the fact that the neighbouring fuel cells are influenced by these irregularities [15]. It is therefore mandatory

- to have a good diagnostics available by which irregularities of the currents occurring at one cell can be detected, opening the possibility for changing parameters and thus reducing the irregularities;
- to find some means to effectively suppress the tendency for irregularities.

Flooding effects in both the cathode flow fields and the gas diffusion layer [16] prevent the reactants from reaching the catalyst. Therefore, no reaction can take place and the current density vanishes at the reactant-free locations. There are many more effects, which cause inhomogeneous current densities in a MEA [17]. Extremely inhomogeneous current densities lead to local high heat production, which can destroy the membrane, whereas a too low current density can lead to a negative cell voltage (cell inversion) that can also destroy the cell [18].

For a single cell some diagnostic methods to gain knowledge about the current density distribution are known. Three methods have been presented by Stumper *et al.* [19], the partial MEA approach, the sub-cell method and the current distribution mapping. The last method is the most advanced one of these three, because it provides a high-resolution current density map by measuring the current directly at many locations of the cell. Although this method is highly advanced, it can only be applied to a single fuel cell and is not eligible to be applied to a fuel cell in a commercial product. Diagnostic methods that can be applied to a fuel cell stack are the electrochemical impedance spectroscopy (EIS) [20,21] and the current interruption method [22]. By these methods one can gain knowledge about different kinds of defects in a particular fuel cell of a stack. However, they provide only integrated information for a whole cell. A further possibility consists of measuring the magnetic field and obtaining information about inner currents by applying magnetotomography [23]. At first sight, this method looks very promising, but suffers from the difficulty that the fields to be measured are small (of the order of the magnetic field of the earth). In fact hitherto the method has only been discussed for single cell problems [24,25].

In this paper we have developed a scheme that fulfils both the above requirements [26]. In the present form it is most easily applied to stacks with graphite flow field plates. The idea is simple (cf Figure 1): highly conducting plates (e.g. made of aluminium) positioned between the cells will enforce a smoothing of the normal currents in the MEAs of the cells. (In this paper normal currents denote currents pointing in stack direction. All currents being orthogonal to normal currents are called transverse currents.) However, this smoothing out can only be achieved by non-negligible transverse currents in the plates. Now slits appropriately

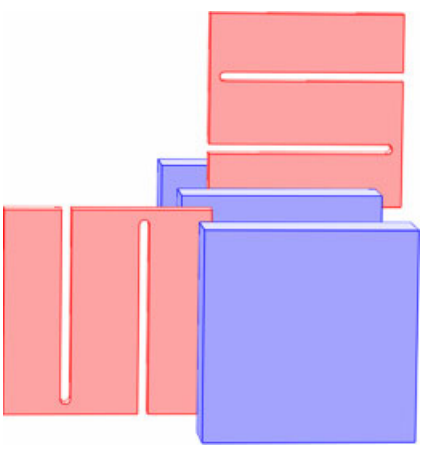

Figure 1. Exploded view of the diagnostic scheme. The full (blue) plates represent individual fuel cells, while the slitted (red) ones represent the metal plates. (For interpretation of color, refer the online version.)

DOI: 10.1002/er

placed in the highly conducting plates should guide these transverse currents to the surface of the stack. At the same time the highly conducting plates should suppress any spreading of irregular currents to the adjacent fuel cells in the assembly.

One possibility for measuring the currents is to guide them at one end of the slit through an external measurement device with a low inner resistance. As an alternative, the currents are guided through an internal connection at the end of the slit and are then detected by means of magneto-tomography. While the first method is better suited for application in laboratories, the second one could be used in commercial products. In this paper we will discuss the first possibility only.

In Section 2 we will apply this scheme to a simple model containing plates of perfect conductivity. We will show that it is possible to get information about the state of individual cells and the location of defects in a cell. In Section 3 we repeat the computations for a realistic stack with realistic parameters. This requires solutions of partial differential equations in three dimensions. The results are discussed in Section 4. It will turn out, that the results of the simple model are usable in many cases at least in first order. On the other hand, the practical applicability and the extent of the smoothing can only be verified and are demonstrated by the numerical computations of Section 3. In the conclusion we discuss the applicability of our scheme to other types of fuel cell stacks.

2. A SIMPLE MODEL

In this section we present a model that in spite of its simplicity contains all the ingredients of the phenomenon. Plates of very high conductivity (e.g. aluminium) are placed between all fuel cells of a stack, cf Figure 2. All plates have the same number N_s of slits dividing the plates into N_s+1 stripes of equal size. These stripes are not electrically isolated from each other. Instead they are connected at their ends in such a way that a transverse current can flow through the plate only by zigzagging through it, touching the border of the plate at locations s_i, cf Figure 2. At these locations the transverse currents can be measured and from that information one can conclude which

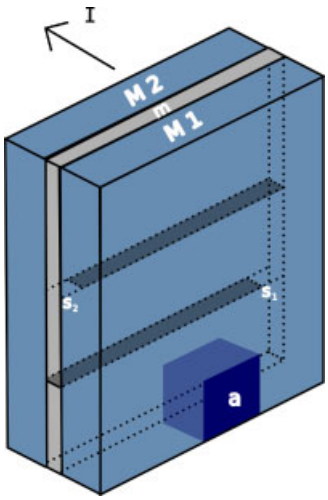

Figure 2. Schematic view showing a plate m of a material (e.g. aluminium) with very high conductivity. The plate is located between the fuel cells $M1$ and $M2$ and split into stripes (slits indicated by shaded areas). The main direction of the current is indicated by an arrow. It is assumed that the MEA of $M1$ has a damaged area, a acting as an insulator. Because of the very high conductivity in m, the current density in each of the cells is practically constant—except in the area a where it is zero. Due to current conservation, transverse currents will rise in m flowing through the connections between the stripes at locations s_1 and s_2.

particular fuel cell and which part of its MEA does not work correctly. The latter information can be obtained as adjacent plates are rotated by 90° and therefore its stripes are perpendicular to those of the previous and next plate (cf. Figure 1).

An example may clarify the phenomenon further: consider one plate m of perfect conductivity m between two fuel cells $M1$ and $M2$ both having an effective MEA area A. Assuming a damaged area a with zero conductivity in the first fuel cell $M1$, the current through this area

$$i = I \cdot \frac{a}{A}, \quad I \text{ is the total electric current} \qquad (1)$$

has now to be distributed over the remaining fuel cell area of $M1$. As the resistance of plate m is assumed to be negligible, the normal component of the current density must be the same everywhere in the remaining fuel cell area of $M1$. This requires a transverse compensation current and because of the slits, part of this current has to pass the

DOI: 10.1002/er

locations s_i. To obtain a homogeneous current density in $M2$, a compensation current of

$$i_Q = \frac{I \cdot a}{(N_S+1) \cdot (A-a)} \tag{2}$$

has to flow from each intact stripe via the metal plate m to the defective one (a derivation for the characteristic current i_Q can be found in [27]). In the case of two slits in the plate m, as shown in Figure 2, two different currents are detected, one at s_1 the other one at s_2. If the damaged area is e.g. in the lower part of the MEA (cf. Figure 2) the currents are

$$i_{s_1} = 2 \cdot i_Q \tag{3}$$

and

$$i_{s_2} = i_Q \tag{4}$$

As expected, the magnitude of the current at a location s_i changes with the size of the damaged area. If the damage occurs at another location, the relations between the currents change as well of course. The results are given in Table I. As can be seen from Table I, in the case under consideration a unique relation exists between the position of a localized damage and the currents i_{s_1} and i_{s_2}. In fact from the values we can infer how significant the damage is and in which stripe of the MEA (defined by the stripes of plate m) the damage has appeared. A corresponding analysis done at the previous plate m' (not shown in Figure 2) provides the information, in which stripe of $M1$ (this time defined by the plate m') the damage has occurred. As the stripes of plate m' are perpendicular to the stripes of m they together divide the MEA area of $M1$ into nine rectangles. From the surface currents connecting the stripes it can thus be inferred in which of the nine rectangles the damage is located and how big it is.

It should be mentioned that the situation becomes more complex if the damage is not local but extended or if several local damages occur at the same time. All these cases will be discussed in a another paper [28].

Table I. Ratio of the currents at locations s_1 and s_2 for the ideal system with negligible resistance of the m plate.

Damage position	i_{s_1}/i_{s_2}
Top	0.5
Middle	−1.0
Bottom	2.0

Besides presenting novel diagnostic possibilities, the additional plates have the additional effect of suppressing all inhomogeneous currents caused by a somehow erratic or not correctly working fuel cell. These are smoothed out at once, avoiding any peak currents at the damaged cell as well as at the adjacent cells. Thus, a much more stable and therefore a much more reliable operation of the fuel cell stack is predicted.

The simple model does not present estimates how well this scheme will work in reality. For example, a competition between currents migrating through the graphite layers and those in the plates will take place and reduce the currents at the locations s_i. The simple model does not contain information how strong this effect is and whether or not currents at the locations are still measurable in practice in spite of this effect. A realistic answer to these questions requires detailed numerical computations. These have been done and the numerical procedure as well as their results will be presented in the next two sections.

3. NUMERICAL SIMULATIONS

For the investigation of the current distribution in a realistic fuel cell stack with aluminium plates between the cells, the system shown in Figure 3 is used. The double slitted metal plate in the centre of the system is embedded between two fuel cells with variable damages. The size of the MEA is about 200 mm × 180 mm × 1 mm; the aluminium and graphite plates are 1 mm thick. The slits are drawn through the total length of the metal plate and are connected by an external wire. The slits width is 1 mm as well.

As we are only interested in stationary solutions, the current conservation

$$\operatorname{div} \vec{j} = 0 \tag{5}$$

has to be obeyed. By using the local Ohm's law $\vec{j} = \sigma \cdot \vec{E}$ with the electric field substituted by the gradient of the potential $\vec{E} = -\operatorname{grad} \phi$ one gets a second order elliptic partial differential equation

DOI: 10.1002/er

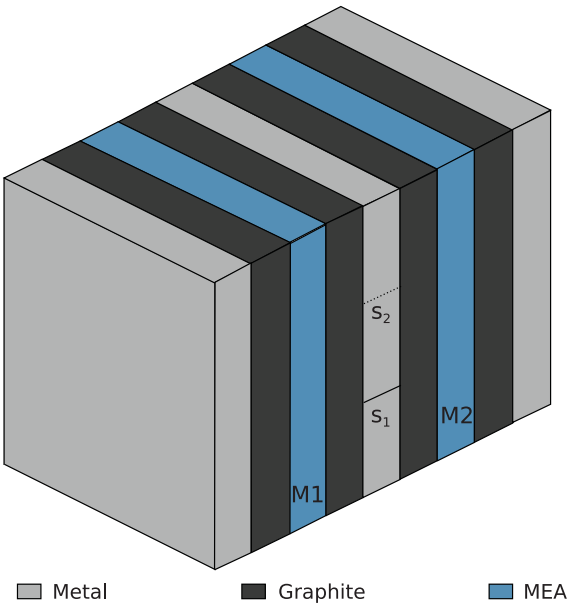

Figure 3. Sketch of the arrangement being used for numerical calculations. The slitted aluminium plate is sandwiched between two fuel cells. Each MEA of these is surrounded by two flow field plates. The system is confined at both ends by aluminium plates, on whose outer planes constant Neumann boundary conditions of about 166 mA/cm^2 are defined. Everywhere else the Neumann boundary conditions are zero. The size of the MEA and that of each plate is 200 mm × 180 mm × 1 mm. The thickness of the slits is set to 1 mm. The connection of the upper slit s_2 is placed on the opposite side of the aluminium plate (indicated by the dotted line).

for the electric potential ϕ.

$$-\operatorname{div}(\sigma \cdot \operatorname{grad} \phi) = 0 \tag{6}$$

Solving this equation is a three dimensional boundary value problem. In this simulation we have used constant Neumann boundary conditions $\vec{j}_n$ on the outer surfaces of the arrangement as shown in Figure 3.

$$\sigma \frac{\partial \phi}{\partial \vec{n}} = -\vec{j}_n, \quad \vec{n} \text{ is the surface normal vector} \tag{7}$$

Using only Neumann boundary conditions, the solution is unique up to a constant. To solve this boundary problem in detail, the three dimensional finite volume method has been chosen, because it fulfils the discretized Maxwell equations.

The value of the homogeneous current density on the outer surfaces of the aluminium plates at the leftmost and rightmost position is set to 166 mA/cm^2, which corresponds to a total electric current of $I = 60$ A. This is appropriate for a DMFC, but because the model is linear in the current, the results carry over to different types of fuel cells with higher currents.

For the slits, Neumann boundary conditions have been chosen as well: the normal currents are set to zero except at the connection points, where the boundary conditions are chosen such, that they are consistent with a given resistance between these points. These are located by a narrow margin above and below the slits.

The aluminium conductivity is 4×10^7 S m^{-1}, while the conductivity of the undamaged MEA is the derivative $\partial j/\partial U$ of the characteristic curve $j(U)$ at an operating point. This is analogous to the determination of the internal conductivity of batteries. For a current density of 166 mA/cm^2 the voltage drop is usually 0.3 V [29]. By these conditions the conductivity is set to 4.33 S m^{-1} (we can neglect possible anisotropies in σ). To simulate damages in the MEAs, the conductivity of arbitrary areas in the MEA can be set to lower values. In this simulation we set the conductivity to 10^{-5} S m^{-1} for one ninth of the entire MEA area. This is modelled for three different defect locations. By applying these values to Equation (2), this leads to a current value of $i_Q = 2.5$ A.

In further calculations, we investigated the impact of a defect on the current density distributions in both the defective MEA itself and the neighbouring MEAs. For this calculation the damage size is set to one third of the MEA area.

Furthermore a fuel cell structure with metallic flow field plates has been calculated. As the conductivity of the stainless steel ($\sigma_{st} = 1.36 \times 10^6$ S m^{-1}) is rather high, it is not possible to measure the transverse compensation currents in an additional slitted aluminium plate. Thus, the slits are directly cut into the flow field plate. For these computations the arrangement shown in Figure 3 is modified, with the graphite plates removed and the aluminium replaced by steel plates.

Our simulations yield the current distribution and by that the exact value of the currents at the slits for various graphite plates (cf. Table II).

DOI: 10.1002/er

Table II. List of transverse and normal conductivities, $\sigma_\perp$ and $\sigma_\parallel$, representing typical materials being used for flow field plates of low and medium temperature fuel cells in addition to the conductivity of aluminium and stainless steel.

	$\sigma_\perp$ (S m^{-1})	$\sigma_\parallel$ (S m^{-1})
Isotropic graphite	4.20×10^3	4.20×10^3
Sigracet PPG 86	5.55×10^3	1.80×10^3
Sigracet BMA 5	1.00×10^4	2.00×10^3
Sigracet BBP 4	2.00×10^4	4.20×10^3
Sigraflex	1.25×10^5	1.70×10^3
Steel	1.36×10^6	1.36×10^6
Aluminium	4.00×10^7	4.00×10^7

4. RESULTS AND DISCUSSION

As already mentioned, the major drawback of the simple model is that it gives only upper limits for the currents at the locations s_i, which may be overly optimistic. To clarify this important issue, a representative resistance of the connection has to be found for each type of the flow field plates. In any electronic device such a resistance is given by that one leading to maximal loss of power at the connection and representing an upper limit that should not be exceeded by measurement devices. The corresponding resistances R_s are listed in Table III. The results can be summarized by the statement that the values lie in a range a modern low cost electronic instrument can easily manage. This proves the applicability of our method.

Table III shows the results for the different materials, computed with the representative resistances. This shows, that the simple model (cf. Table I) gives a surprisingly good approximation to the realistic computations (cf Table III). The reason for this is the high conductivity of aluminium and the small (effective) conductivity of the MEAs.[1] Therefore, damages in a MEA lead to transverse currents between the aluminium stripes that can be rather well estimated by the simple model. Of course the simple model is unable to predict how much of these currents will pass the locations s_i where the stripes are connected. Indeed currents can bypass a slit between two stripes by diving into the graphite and returning into the aluminium. However, because of the high conductivity of aluminium, this happens along the whole length of the slit and gives rise to a resistance being (a) rather independent of the location of the damage in a stripe and (b) nearly the same for all stripes. Thus the ratios of the currents passing the locations s_i should be very similar to those of the simple model. Of course getting the absolute values of these currents requires extensive numerical computations for each material. We have done these calculations and determined the averaged fraction α of the transverse currents passing the locations s_i. The smaller α the more difficult the measurements are. We think that $\alpha \gtrsim 0.3$ is acceptable for standard measuring devices. The computed α values are shown in Table III.

Table III. Ratio of the currents in the aluminium plate at locations s_1 and s_2 (cf Figure 3) compared for various graphite flow field plates.

	Damage position	i_{s_1}/i_{s_2}
Isotropic graphite	Top	0.48
$R_s = 2.09 \times 10^{-3}\,\Omega$	Middle	−1.0
$\alpha = 0.47$	Bottom	2.09
Sigracet PPG 86	Top	0.48
$R_s = 1.95 \times 10^{-3}\,\Omega$	Middle	−1.0
$\alpha = 0.46$	Bottom	2.08
Sigracet BMA 5	Top	0.49
$R_s = 1.33 \times 10^{-3}\,\Omega$	Middle	−1.0
$\alpha = 0.45$	Bottom	2.03
Sigracet BBP 4	Top	0.49
$R_s = 0.73 \times 10^{-3}\,\Omega$	Middle	−1.0
$\alpha = 0.42$	Bottom	2.01
Sigraflex	Top	0.53
$R_s = 0.39 \times 10^{-3}\,\Omega$	Middle	−1.0
$\alpha = 0.35$	Bottom	1.89
Steel	Top	0.22
$R_s = 16.7 \times 10^{-3}\,\Omega$	Middle	−1.0
$\alpha = 0.43$	Bottom	4.48

In the last case, the slit is directly cut into the steel flow field plate.

We have made computations for PEMFCs with steel flow field plates. To apply our scheme to this type of fuel cells, the slits have to be cut directly in the flow fields. As stainless steel has a conductivity much lower than aluminium, it is no surprise that

[1]The thin-gas diffusion layer can also be included into the calculations. In spite of having a relatively high transverse conductivity, an estimate [27] shows, that the effect is negligible in realistic cases.

DOI: 10.1002/er

the results differ considerably from those of the simple model. Nevertheless the high R_s value in Table III documents the possible applicability of our method for steel flow fields.

It is quite normal that even a well functioning fuel cell has a locally varying current density. These variations may be static or dynamic [13]. For a single cell, these variations may be unproblematic, but the situation in the stack can be quite different as these variations can accumulate. The situation may become worse if one or more fuel cells are damaged in certain areas of their MEA but still doing their jobs. For avoiding accumulations in all these cases it is mandatory not to allow any irregularity of one cell to influence the next or the previous one. We have investigated this problem by computing an arrangement of a damaged fuel cell followed by an intact one. We discuss two cases:

(a) *Situation without aluminium plates* (cf Figure 4):

(Computations have been done for flow field plates fabricated from Sigracet PPG 86 graphite.) The stack is taken into account by assuming that a homogeneous current enters the flow field plates before the first fuel cell and a homogeneous current is leaving the flow field plates after having passed the second fuel cell. We simulate a worst-case scenario, namely a massive failure in the MEA of fuel cell $M1$ with the result that the upper third of the MEA does not produce current at all.[2] The result is shown in Figure 4(a). A strong peak of the current density appears next to the damaged area in the MEA of fuel cell $M1$. Such a peak will probably lead to a fast expansion of the damage [15]. Furthermore, as can be seen from Figure 4(b), a steep dip at the same location appears in the MEA of fuel cell $M2$. Although this cell is undamaged, this dip will lead to increased degradation of the second MEA. Deducing from our calculations and the calculations in [15] one has to be afraid of a chain reaction leading to more and more ill-working cells in the stack.

[2]Depending on the flow field structure, a defective supply line or accumulated water in the flow field can lead to such a massive failure without directly damaging the MEA.

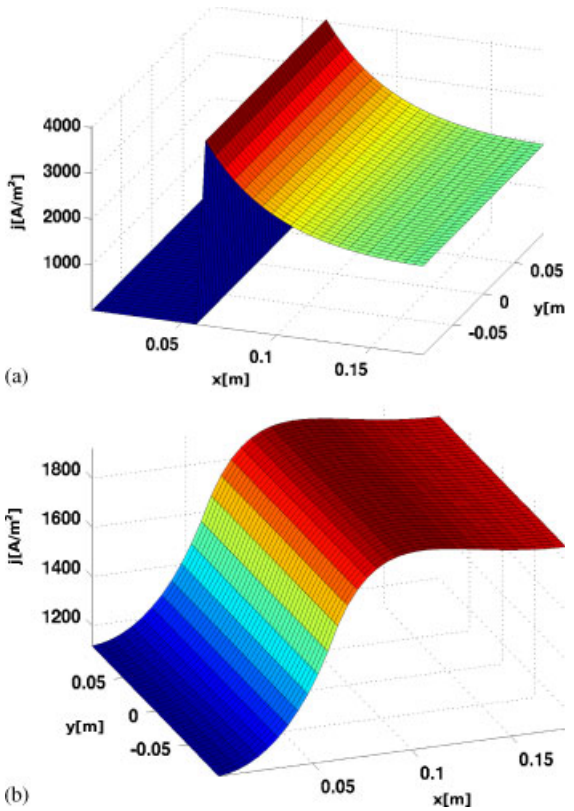

Figure 4. Normal current density in the MEAs of two successive fuel cells in a stack. The arrangement is that of Figure 3, where the slitted aluminium plate is removed and the two non-slitted aluminium plates have been replaced by graphite flow field plates. Note the enormous peak close to the damaged area of the first MEA (a) and a steep dip in the MEA of the second fuel cell although its MEA is not damaged (b). Obviously there is a possibility of a chain reaction.

(b) *Situation with aluminium plates* (cf Figure 5):

The stack is taken into account by assuming that a homogeneous current enters the aluminium plate before the flow field plate of the first fuel cell and a homogeneous current is leaving after having passed the second fuel cell, its flow field plates and the aluminium plate. For this calculations we omitted the slits in the aluminium plate, as they are of minor relevance for the homogenization effect. For the same damage in the MEA $M1$ as before the result is shown in Figure 5. Now peaks of the electric current cannot be detected, neither in the

DOI: 10.1002/er

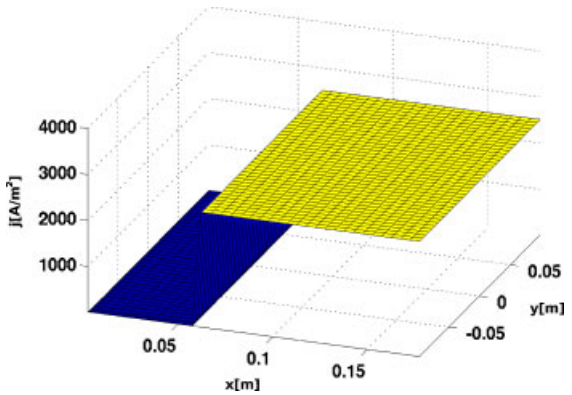

Figure 5. Normal current density in the MEAs of a damaged fuel cell in a stack. The arrangement is that of Figure 3, only the slits are left out for simplicity. (Their effect is not of relevance here). Note, that the peak has vanished. The current density distribution of the next fuel cell in series is totally homogeneous (not shown). Obviously the damage can neither extend in the first cell nor spread into the undamaged cell, although the first cell is already heavily affected.

first (cf. Figure 5) nor in the second fuel cell in spite of the heavy damage in the first cell.

It should be noted here, that the peak and the steep dip are qualitatively the same for all graphite flow field plates, with one exception: For flow field plates fabricated from Sigraflex graphite the peaks are already strongly suppressed, changing the current density only by $\pm 10\%$ in our calculations. But this result should be treated with caution because the channels in the flow field plates were not taken into account.

More detailed computations of the defect expansion, including 15 fuel cells in the arrangement, can be found in [27]. As in the computation presented here the current density in the MEAs is decoupled by the metal plates confining the arrangement, no major difference to the detailed computations can be found.

It might seem, that our scheme does not work for the first and the last cell in the stack. However, adding a dummy cell, i.e. a plate with medium conductivity at the front and at the back of the stack enables diagnosis for these cells as well. We have estimated the power loss and have found that it amounts to 1–3 W per dummy cell. Thus, when using the dummy cell trick, diagnostics with our scheme becomes possible even for a single cell.

As further plates are added into the fuel cell stack, further contact resistances will occur. These cannot be estimated by the numerical program, therefore no values can be given. Although further contact resistances are undesired for the stack operation, they might increase the measurable transverse current in the aluminium plate.

It should be mentioned that our scheme fails if the MEA of a cell begins to degrade all over its area in exactly the same manner. As this case is extremely improbable, we have not discussed it further in this context.

5. CONCLUSION

For graphite flow field plates we have shown: placing slitted 1 mm aluminium plates between the flow field plates of adjacent fuel cells in a stack—which elongates a 100 cell stack by about 10 cm—it is possible

- to localize damaged areas in the MEA of the fuel cells and to determine how serious the damage is. This is done by forcing inner irregular currents to appear at the surface of the stack where they can be measured.
- to smoothen inhomogeneities of currents in every MEA and prevent irregularities in one MEA to induce irregularities in the MEA of the next and previous fuel cell, which otherwise could lead to a destructive chain reaction.

Our method is applicable to fuel cells with flow field plates made of low conductivity material (graphite). Some types of fuel cells, e.g. the SOFC type, are using metallic flow field plates. In this case our scheme cannot be applied directly. However, if slits are cut into the flow field plates directly and gaps caused by this procedure are closed with an insulating material then—as our calculations have shown for metallic flow field plates—there is no principle reason why our scheme should not work as well. In this work we have investigated simple defects and demonstrated that these can be uniquely detected. However, realistic defects such as catalyst degradation, flooding of cathode flow fields or of diffusion

DOI: 10.1002/er

layers have a more complex structure. To find out if our scheme can detect these kinds of defects, a more detailed investigation, including the theory of tomography, needs to be done. Certainly, this is beyond the scope of this paper, but is discussed in a different paper [28].

Experiments corroborating the applicability of our scheme are done right now and results will be published as soon as they are available.

NOMENCLATURE

$M1, M2$	= MEA1, MEA2
m	= slitted metal plate
N_s	= Number of slits in m
s_1, s_2	= connections between stripes
i_{s_1}, i_{s_2}	= currents through s_1 and s_2
A	= MEA area
a	= size of defect
I	= total electric current
i_Q	= characteristic current
$\vec{j}$	= current density
σ	= conductivity
$\vec{E}$	= electric field
ϕ	= lectric potential
$\vec{n}$	= surface vector
$\vec{j}_n$	= surface current density
$\sigma_\perp$	= transverse conductivity
$\sigma_\parallel$	= normal conductivity
R_s	= connection resistance
α	= reduction factor

ACKNOWLEDGEMENTS

We would like to thank A. Egmen, A.A. Kulikovsky, M. Müller and K. Wippermann for stimulating discussions and J. Mergel for encouraging this work.

REFERENCES

1. Wind J, Spah R, Kaiser W, Bohm G. Metallic bipolar plates for PEM fuel cells. *Journal of Power Sources* 2002; **105**:256–260.
2. Larminie J, Dicks A. *Fuel Cell Systems Explained*. Wiley: West Sussex, 2003.
3. Dohle H, Schmitz H, Bewer T, Mergel J, Stolten D. Development of a compact 500 W class direct methanol fuel cell stack. *Journal of Power Sources* 2002; **106**: 313–322.
4. Heinzel A, Nolte R, Ledjeff-Hey K, Zedda M. Membrane fuel cells—concepts and system design. *Electrochimica Acta* 1998; **43**:3817–3820.
5. Mikkola M. Experimental studies on polymer electrolyte membrane fuel cell stacks. *Master Thesis*, Helsinki University of Technology, 2001.
6. Wang L, Husar A, Zhou T, Liu H. A parametric study of PEM fuel cell performances. *International Journal of Hydrogen Energy* 2003; **28**:1263–1272.
7. Tüber K, Pócza D, Hebling C. Visualization of water buildup in the cathode of a transparent PEM fuel cell. *Journal of Power Sources* 2003; **124**:403–414.
8. Tüber K, Zobel M, Schmidt H, Hebling C. A polymer electrolyte membrane fuel cell system for powering portable computers. *Journal of Power Sources* 2003; **122**:1–8.
9. Scott K, Taama WM, Argyropoulos P. Engineering aspects of the direct methanol fuel cell system. *Journal of Power Sources* 1999; **79**:43–59.
10. Zamel N, Li X. Non-isothermal multi-phase modeling of PEM fuel cell cathode. *International Journal of Energy Research* 2009; DOI: 10.1002/er.1572.
11. Yoon YG, Lee WY, Yang TH, Park GG, Kim CS. Current distribution in a single cell of PEMFC. *Journal of Power Sources* 2003; **118**:193–199.
12. Noponen M, Mennoloa T, Mikkola M, Hottinen T, Lund P. Measurement of current distribution in a free-breathing PEMFC. *Journal of Power Sources* 2002; **106**: 304–312.
13. Wippermann K. Private communication.
14. Su A, Chiu YC, Weng FB. The impact of flow field pattern on concentration and performance in PEMFC. *International Journal of Energy Research* 2005; **29**: 409–425.
15. Kulikovsky AA. Electrostatic broadening of current-free spots in a fuel cell stack: the mechanism of stack aging? *Electrochemistry Communications* 2006; **8**:1225–1228.
16. Hekenjos A, Muenter H, Wittstadt U, Hebling C. A PEM fuel cell for combined measurement of current and temperature distribution, and flow field flooding. *Journal of Power Sources* 2004; **131**:213–216.
17. Le Canut JM, Abouatallah RM, Harrington DA. Detection of membrane drying, fuel cell flooding, and anode catalyst poisoning on PEMFC stacks by electrochemical impedance spectroscopy. *Journal of the Electrochemical Society* 2006; **153**:A857–A864.
18. Mulder G, Ridder FD, Coenen P, Weyen D, Martens A. Evaluation of an on-site cell voltage monitor for fuel cell systems. *International Journal of Hydrogen Energy* 2008; **33**:5728–5737.
19. Stumper J, Campbell SA, Wilkinson DP, Johnson MC, Davis M. In-situ methods for the determination of current distributions in PEM fuel cells. *Electrochimica Acta* 1998; **43**:3773–3783.
20. Yuan X, Sun JC, Wang H, Zhang J. AC impedance diagnosis of a 500 W PEM fuel cell stack part II: individual cell impedance. *Journal of Power Sources* 2006; **161**(2):929–937.
21. Gomadam PM, Weidnern JW. Analysis of electrochemical impedance spectroscopy in proton exchange membrane fuel cells. *International Journal of Energy Research* 2005; **29**:1133–1151.

22. Mennola T, Mikkola M, Noponen M, Hottinen T, Lund P. Measurement of ohmic voltage losses in individual cells of a PEMFC stack. *Journal of Power Sources* 2002; **112**:261–272.
23. Lustfeld H, Reißel M, Schmidt U, Steffen B. Reconstruction of electric currents in a fuel Cell by magnetic field measurements. *Journal of Fuel Cell Science and Technology* 2009; **6**:021012.
24. Hauer KH, Potthast R. Magnetic tomography for fuel cells—current status and problems. *Journal of Physics*: *Conference Series* 2007; **73**(1):012008.
25. Hauer KH, Potthast R, Wannert M. Algorithms for magnetic tomography—on the role of a priori knowledge and constraints. *Inverse Problems* 2008; **24**: 045008.
26. Lustfeld H, Reißel M, Steffen B. Defektkontrolle für ein oder mehrere elektrische Betriebselemente. German patent application DE: 102007061642.4-35 (20.12.2007).
27. Hirschfeld J. Tomographic problems in the diagnostics of fuel cell stacks. *Diploma Thesis*, Jül-Report Jül-4291 Forschungszentrum Jülich: Jülich, 2009. http://hdl.handle.net/2128/3588.
28. Hirschfeld JA, Lustfeld H, Reißel M, Steffen B. Tomographic diagnostics of current distributions in a fuel cell stack. *International Journal of Energy Research* 2009; DOI: 10.1002/er.1634.
29. Dohle H. Entwicklung und Modellierung von Direkt-Methanol-Brennstoffzellen. *Ph.D. Thesis*, Jül report Jül-3752, Forschungszentrum Jülich: Jülich, 2000.